SPACE-TO-SPACE BASED RELATIVE MOTION ESTIMATION USING DIRECT RELATIVE ORBIT PARAMETERS

Trevor Bennett and Hanspeter Schaub

Advanced Maui Optical and Space Surveillance (AMOS) Technologies Conference

Wailea, Maui, Hawaii September 15–18, 2015

SPACE-TO-SPACE BASED RELATIVE MOTION ESTIMATION USING LINEARIZED RELATIVE ORBIT ELEMENTS

Trevor Bennett* **and Hanspeter Schaub**†

Many methods of relative motion estimation involve the direct estimation of time-evolving position and velocity variables. Proposed is an alternate approach where the constants of integration in the Clohessy-Wiltshire equations are considered as the state variables. The mapping and equations of motion are developed for the new state variables which accommodate perturbation and control accelerations. The under-determined angles-only relative orbit Extended Kalman filter (EKF) navigation approach is used to estimate non-dimensional linearized relative orbit elements (LROEs). Estimating LROEs enables the relative orbit geometry to be directly determined. For the angles-only implementation, the relative orbit scale is undetermined, but the proposed non-dimensional LROEs elegantly allow for the relative orbit shape to be estimated.

INTRODUCTION

There is an increasing interest in space-based space situational awareness around satellite assets in the tracking of orbital debris or target objects. The relative position of the target object can be estimated using relative motion description estimation or inertial methods such as ground based estimation and inertial differencing with GPS measurements.[1,2] Of particular interest is the space-based tracking of objects near critical circular orbit regimes, for example near the Geostationary belt or the International Space Station. This manuscript addresses estimation of the relative motion about circular chief orbits.

Researches have investigated estimation of the relative motion through a variety of state descriptions. One approach is to difference the orbit elements to derive new parameter sets.[1,3] Expressing the relative motion estimation in polar coordinates has also been considered.[4] More common relative motion descriptions such as the Clohessy-Wiltshire (CW) equations describe the motion using time-varying Cartesian or curvilinear coordinates.[5] Research into using the CW equations for relative motion estimation has led researchers to derive new parameterizations.[3,6–8] The observability of estimating the Cartesian state using the CW formulation has also been considered demonstrating the restrictions in applying the equations directly in estimation.[9] Further exploration has utilized curvilinear and nonlinear transformations of the linearized motion, however the formulations suffer from the same drawbacks of other relative motion descriptions.[10] However, to date the estimation methodology has assumed a Cartesian or orbit element difference state vector as outlined in[11] including time-varying additional term derivations. Proposed is a novel relative motion state vector derived from the invariants of motion that reside in the classical Clohessy-Wiltshire equations.

*Graduate Research Assistant, Aerospace Engineering Sciences, University of Colorado.

†Professor, Department of Aerospace Engineering Sciences, University of Colorado, 431 UCB, Colorado Center for Astrodynamics Research, Boulder, CO 80309-0431

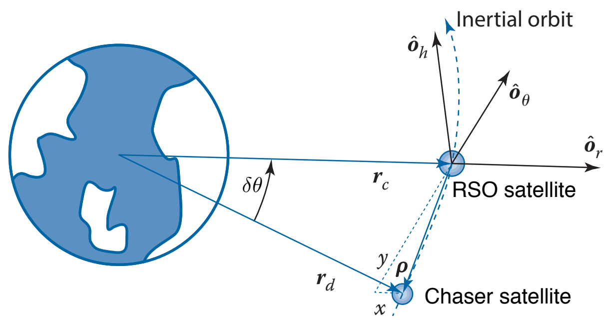

Figure 1. Local vertical local horizontal rotating Hill frame for formation flying.

Linearized Relative Orbit Elements (LROEs) employ invariants of the linearized relative motion provided by the CW equations. Present in the CW equations are shape parameters that describe the size and location of the relative orbit. The present study uses these constant shape parameters, or LROEs, as the state vector for the estimation scheme. An inverse mapping and the equations of motion are available for these parameters using variational equation techniques.[12] The LROE differential equations enable the relative orbit to be directly propagated including perturbation forces such as differential drag and coulomb formations studied by other authors.[13,14] Implementing a relative motion filter with a set of constants mimics an epoch state filter which has been studied in low-Earth orbit (LE0) applications.[15] There also exists substantial evaluation techniques for the covariance of epoch state filters.[16] With support of epoch state Kalman filtering methodology, utilization of the invariant-inspired relative motion parameters exhibits exciting applications in relative motion sensing and control.

This paper provides the development of the LROE based extended Kalman filter for estimation of relative motion about a circular chief. The challenging angles-only relative motion estimation problem studied in References 1 and 9 is not fully observable. It is impossible to distinguish with angles-only measurements between 2 relative orbits that differ only by a common scaling factor. Therefore, it is of interest to showcase the geometric-insight advantages of the LROE formulation within the challenges of angles-only estimation problems. Of interest is how the angle-only problem can be reformulated using non-dimensional LROE's to make the relative orbit shape, not the scale, observable. The motivation for such work is that it allows for elegant relative orbit control laws to be developed in terms of LROE that directly control the relative trajectory shape. Several CubeSat missions have implemented relative motion control schemes that would benefit from the presented estimation approaches.[17–19] For example, the control of a drifting safety-ellipse needs to strongly control the oscillatory out-of-plane and in-plan oscillatory motion, but only looses needs to control the along-track drift rate. With LROE estimation simple feedback controls are enabled to selectively control relative orbit shape aspects.

LINEARIZED RELATIVE ORBIT ELEMENTS

The relative motion of two satellites can be described by the inertial state vector difference in the deputy, or target, and chief. Consider the Hill frame[20] defined in Figure 1. The relative position is given by the inertial difference

$$\boldsymbol{\rho} = \boldsymbol{r}_{\text{deputy}} - \boldsymbol{r}_{\text{chief}} \tag{1}$$

The relative position $\boldsymbol{\rho}$ and the relative velocity $\dot{\boldsymbol{\rho}}$ are the desired parameters for relative motion estimation. For small relative positions that reside within 1 km of the chief orbit, the relative motion can be linearized about the chief orbit. The linearized form can be further reduced to the well known Clohessy-Wiltshire (CW) equations by further assuming the chief orbit is circular and solving for the analytic solution. The CW equations provide a convenient form for directly prescribing the relative orbit and are often utilized for geometric insight. The Hill frame position vector components are given by[20,21]

$$x(t) = A_0 \cos(nt + \alpha) + x_{\text{off}} \tag{2a}$$

$$y(t) = -2A_0 \sin(nt + \alpha) - \frac{3}{2} nt x_{\text{off}} + y_{\text{off}} \tag{2b}$$

$$z(t) = B_0 \cos(nt + \beta) \tag{2c}$$

where A_0 and B_0 are the amplitudes of the cyclic in-plane and out-of-plane motion, α and β are the associated phase angles, and x_{off} and y_{off} are the orbit radial and along-track offsets. The relative state vector is characterized by the 6 invariants $(A_0, \alpha, B_0, \beta, x_{\text{off}}, y_{\text{off}})$ of the unperturbed motion. These invariants, or Relative Orbit Elements (ROEs), provide convenient scaling and phasing terms enable direct shaping of the relative orbit. It is the intuitive nature of these constants that motivates the following development. Other ROEs could be used such as the initial Hill frame position and velocity coordinates, but this paper will focus on ROEs that provide very convenient geometric insight into the relative orbit geometry. As this set of ROEs is derived from the linearized relative motion solution, the invariant vector of the CW equations is referred to as a Linearized ROE or LROE.

If the elliptical invariant A_0 or B_0 are zero in Eq. (2), then the angles α and β are ambiguous and lack influence.[12] Without modification, the CW equations therefore are unable to provide a unique solutions to some cases including the Leader-Follower configuration. A non-singular CW equation form is introduced in 12 that avoids ambiguity.

NONSINGULAR MODIFICATION TO THE LROE SET

A slight modification to the CW equations removes the α and β ambiguity and largely preserves the inherent insight.[12] The modified set of LROEs that utilizes the trigonometric expansions

$$\begin{aligned} A_0 \cos(\alpha + nt) &= A_0 \cos(\alpha) \cos(nt) - A_0 \sin(\alpha) \sin(nt) \\ A_0 \sin(\alpha + nt) &= A_0 \sin(\alpha) \cos(nt) + A_0 \cos(\alpha) \sin(nt) \\ B_0 \cos(\alpha + nt) &= B_0 \cos(\alpha) \cos(nt) - B_0 \sin(\alpha) \sin(nt) \end{aligned}$$

where the new shape constants A_1, A_2, B_1, and B_2 are defined as

$$A_1 = A_0 \cos(\alpha) \qquad A_2 = A_0 \sin(\alpha) \qquad B_1 = B_0 \cos(\alpha) \qquad B_2 = B_0 \sin(\alpha) \tag{4}$$

The ambiguity of the linear combination of A_0 and α, or B_0 and β, is removed in place of two perpendicular scaling terms. The modified non-singular LROE set therefore becomes

$$x(t) = A_1 \cos(nt) - A_2 \sin(nt) + x_{\text{off}} \tag{5a}$$

$$y(t) = -2A_1 \sin(nt) - 2A_2 \cos(nt) - \frac{3}{2} nt x_{\text{off}} + y_{\text{off}} \tag{5b}$$

$$z(t) = B_1 \cos(nt) - B_2 \sin(nt) \tag{5c}$$

LROEs both in the traditional and nonsingular forms provide the relative motion geometry in the absence of perturbation. In the absence of perturbations, these parameters remain constant. In the presence of perturbations, a Lagrangian Bracket formulation may be used to generate the specific LROE evolution equations.[12]

LROE DYNAMICS USING LAGRANGIAN BRACKETS

The dynamics of the state vector are required for navigation filter applications. As described, the LROE set is considered to be invariant while the spacecraft pairs are influenced only by two-body gravitational effects. However, more accuracy to the dynamic modeling and filter applicability requires additional forces or perturbations to drive the LROE evolution. First derived in Reference 12, the dynamics of the LROE state can be obtained by applying Lagrange Brackets to the non-singular LROE equations. This approach is analogous to Lagrange's planetary equations in that the LROE set becomes osculating to match the perturbed relative orbit. The nominally invariant LROE set $\boldsymbol{X}$, defined as

$$\boldsymbol{X} = (A_1, A_2, B_1, B_2, x_{\text{off}}, y_{\text{off}}) \tag{6}$$

evolves according to Eq. (7) where $\boldsymbol{a}_d$ is the disturbance acceleration in the Hill frame.[12]

$$\dot{\boldsymbol{X}} = \underbrace{\begin{bmatrix} \frac{-7\sin(nt)}{n} & \frac{-2\cos(nt)}{n} & 0 \\ \frac{-7\cos(nt)}{n} & \frac{2\alpha_2\cos(nt)-6(nt-1)\sin(nt)}{n} & 0 \\ 0 & 0 & \frac{-\sin(nt)}{n} \\ 0 & 0 & \frac{\cos(nt)}{n} \\ \frac{-4\sin(2nt)}{n} & \frac{18}{n} & 0 \\ \frac{\alpha_2+2+\alpha_1(\cos(2nt)-\sin(2nt))}{n} & \frac{-3\alpha_2+4+2\alpha_2(\cos(2nt)+\sin(2nt))}{n} & 0 \end{bmatrix}}_{B(\boldsymbol{X},t)} \begin{bmatrix} a_x \\ a_y \\ a_z \end{bmatrix} \tag{7}$$

where the simplifying terms α_1 and α_2 are defined as

$$\alpha_1 = 3nt - 4 \tag{8a}$$

$$\alpha_2 = 3nt + 4 \tag{8b}$$

Eq. (7) is the variational equation of the non-singular LROE set, and is the relative motion equivalent of Gauss' variational equation for inertial orbital motion. Any perturbation or control accelerations can be applied to propagate the LROE variations. Recall that the CW equations already account for two-body motion, so the differential perturbation accelerations can include drag, solar radiation pressure, and higher order gravity.

LROE FILTER FORMULATION

Using the non-singular LROE set as the state variables, the relative orbit can be determined through a sequential estimation scheme. An extended Kalman filter (EKF) is applied to estimating the LROE set to provide the relative orbit at any time. Motivated by the prevalence of visual cameras in satellites, bearings only measurements are used. The goal of this study is to formulate the LROE-based relative motion estimation problem, and study the observability of the LROE state.

State and Measurement Models

The non-singular LROE set defined in Eq. (6) is used as the state vector for relative motion estimation. Because the LROE relative orbit coordinates are invariants of linearized unperturbed motion, the proposed unperturbed filter formulation is an epoch state filter where the current measurement provides information that is mapped to a prescribed epoch. This filter considers the initialization time as the prescribed epoch. The measurement equations include the time dependence allowing the state to remain constant. The bearing measurement model used is shown in Eq. (10). The bearing measurements can also be written in terms of the state vector variables by using the mappings provided by Eq. (5).

$$\mathrm{Az} = \arctan\left(\frac{y(t)}{x(t)}\right) \tag{9}$$

$$\mathrm{El} = \arctan\left(\frac{z(t)}{\sqrt{x^2(t)+y^2(t)}}\right) \tag{10}$$

The measurements and truth trajectory are generated from the output of an inertial frame simulation. The dynamics include only two body effects for the present study, however both the filter and the LROE formulation are capable of more complicated dynamical models. The truth state is perturbed slightly at every time step using an error provided by a random sampling of the process noise matrix propagated simultaneously with the truth state.

$$\boldsymbol{X}_k^{\text{true}} = \boldsymbol{X}_{k,\text{nominal}}^{\text{true}} + \text{sample}(Q_k) \tag{11}$$

The noise on the measurements appears from 3 sources. The state has unmodeled dynamical error and therefore the true measurements will contain a representative error not included in the propagated filter model. A set of two first order Gauss-Markov variables are propagated and added onto the bearing measurements. The final error is introduced as a Gaussian zero-mean white noise process. Therefore the true azimuth measurement is computed by Eq. (12) and similarly for elevation.

$$\mathrm{Az} = \mathrm{Az}_{\text{exact}} + \sigma_{\text{Az}}^{GM} + w_{\text{Az}} \tag{12}$$

The inclusion of the Gauss-Markov process more accurately represents the expected performance of a visual navigation camera and the white noise provides the random noise source. The first order Gauss-Markov random walk process is propagated using the form

$$\dot{\boldsymbol{\sigma}} = -B_{\text{GM}}\boldsymbol{\sigma} + W_k \tag{13}$$

where the B matrix provides the time-constant-drive decay of the current variable value. The white noise process matrix W_k is a randomly sampled value from a camera specific error covariance W. The time constants for the camera considered are 15 minutes such that the Gauss-Markov B matrix is given by

$$B_{\text{GM}} = \begin{bmatrix} 1/\tau_{\text{Az}} & 0 \\ 0 & 1/\tau_{\text{El}} \end{bmatrix} \tag{14}$$

The W matrix is the diagonal covariance of the camera white noise with elements w_{cam}. The camera considered in this study is a 5 mega-pixel, $n_{\text{p}} = 5 \times 10^6$, camera. The noise w_p is assumed to be about 1 pixel for 1σ error. The camera is assumed to have a more narrow field of view with a half angle of $\alpha = 10°$. This gives the radian noise magnitude of

$$w_{\text{cam}} = \frac{w_p}{n_{\text{p}}} * 2\alpha \tag{15}$$

The noise parameters provides a more realistic baseline for the LROE EKF formulation.

Extended Kalman Filter Formulation

The EKF formulation is a nonlinear approach to a linearized problem. The sequential Kalman filter is suitable for estimating the LROE state vector from a series of bearing measurements motivated by satellite based tracking and estimation. The use of an EKF allows the state estimate to update the current LROE estimate rather than updating a correction term to the initial LROE guess. This is desired for the estimation of constants where the *a priori* is either poor or nearly unknown.

The filter state is propagated forward in time using Eq. (16) where $\boldsymbol{F}$ are the modeled forcing functions. The dynamics are not constrained to be two-body admitting perturbations in the presented filter formulation. The LROE variational equations in Eq. (7) introduce a time-varying LROE set with filter-modeled perturbation forces

$$\dot{\boldsymbol{X}}_k = \boldsymbol{F}(\boldsymbol{X}(t_k), t_k) = B(\boldsymbol{X}(t_k), t_k)\boldsymbol{a}_d \tag{16}$$

The linearized dynamics matrix A is given as the state partials of the modeled forcing function $\boldsymbol{F}$ evaluated at the current LROE set. The A matrix is forcing function dependent and might require numerical approximation for some dynamical models.

$$A = \left[\frac{\partial \boldsymbol{F}(\boldsymbol{X}, t)}{\partial \boldsymbol{X}}\right]^* \tag{17}$$

The presented filter results use two-body unperturbed dynamics and so the A matrix is all zero. The filter does not assume a zero A matrix as seen in the covariance propagation. The state covariance matrix is propagated forward using the state transition matrix form in Eq. (18) with the addition of process noise.

$$\bar{P}_k = \Phi\left(t_k, t_{k-1}\right) P_{k-1} \Phi^T\left(t_k, t_{k-1}\right) + S(t) \tag{18}$$

The process noise matrix S is added at every time step to prevent filter saturation. The process noise for the current step is given by Eq. (19) where Q is the process noise covariance matrix.

$$\dot{S} = AS + SA + Q \tag{19}$$

The linearized filter utilizes the partials of the measurements and of the dynamics to the provided state vector. The linearized measurment model given by $\boldsymbol{H}$ is given by

$$\tilde{\boldsymbol{H}} = \left[\frac{\partial \boldsymbol{G}(\boldsymbol{X}, t)}{\partial \boldsymbol{X}}\right]^*_i = \begin{bmatrix} \frac{\partial \text{Az}}{\partial \boldsymbol{X}} \\ \frac{\partial \text{El}}{\partial \boldsymbol{X}} \end{bmatrix} \tag{20}$$

The Kalman filter uses the time-varying measurement partials matrix $\tilde{\boldsymbol{H}}$ to map the current LROE state into the measurements. The $\tilde{\boldsymbol{H}}$ matrix using the non-singular LROE form using the definitions in Eq. (5) is

$$\tilde{\boldsymbol{H}}_{1,1}(t) = -x^2(t)\left(\frac{2\sin(nt)}{x(t)} - \frac{-y(t)\cos(nt)}{x^2(t)}\right)/\kappa_1 \tag{21a}$$

$$\tilde{\boldsymbol{H}}_{1,2}(t) = -x^2(t)\left(\frac{2\cos(nt)}{x(t)} + \frac{-y(t)\sin(nt)}{x^2(t)}\right)/\kappa_1 \tag{21b}$$

$$\tilde{\boldsymbol{H}}_{1,3}(t) = 0 \tag{21c}$$

$$\tilde{\boldsymbol{H}}_{1,4}(t) = 0 \tag{21d}$$

$$\tilde{\boldsymbol{H}}_{1,5}(t) = x^2(t)\left(\frac{y(t)}{x^2(t)} - \frac{3nt}{2x(t)}\right)/\kappa_1 \tag{21e}$$

$$\tilde{\boldsymbol{H}}_{1,6}(t) = x(t)/\kappa_1 \tag{21f}$$

$$\tilde{\boldsymbol{H}}_{2,1}(t) = -z(t)\left(2x(t)\cos(nt) - 4y(t)\sin(nt)\right)/2\kappa_1\kappa_2 \tag{21g}$$

$$\tilde{\boldsymbol{H}}_{2,2}(t) = z(t)\left(2x(t)\sin(nt) + 4y(t)\cos(nt)\right)/2\kappa_1\kappa_2 \tag{21h}$$

$$\tilde{\boldsymbol{H}}_{2,3}(t) = \cos(nt)/\kappa_2 \tag{21i}$$

$$\tilde{\boldsymbol{H}}_{2,4}(t) = -\sin(nt)/\kappa_2 \tag{21j}$$

$$\tilde{\boldsymbol{H}}_{2,5}(t) = \left(-z(t)(2x(t) - nty(t))\right)/2\kappa_1\kappa_2 \tag{21k}$$

$$\tilde{\boldsymbol{H}}_{2,6}(t) = -2z(t)y(t)/2\kappa_1\kappa_2 \tag{21l}$$

where

$$\kappa_1 = x^2(t) + y(t)^2 \tag{22a}$$

$$\kappa_2 = \sqrt{\kappa_1}\left(\frac{z^2(t)}{\kappa_1} + 1\right) \tag{22b}$$

The Kalman gain is assembled using

$$\bar{K}_k = \bar{P}_k \tilde{H}_k^T \left(\tilde{H}_k \bar{P}_k \tilde{H}_k^T + R_k\right)^{-1} \tag{23}$$

where the measurement error matrix is given by

$$R = k_R W = k_R \begin{bmatrix} w_{\text{cam}} & 0 \\ 0 & w_{\text{cam}} \end{bmatrix} \tag{24}$$

The R matrix is intentionally under-weighted by a factor k_R to encapsulate the unmodeled error sources represented by the Gauss-Markov process and random process in the truth measurements.

The state covariance is updated using the Joseph formulation as shown in Eq. (25). The Joseph formulation of the covariance matrix is more consistently symmetric.

$$P_k = \left[I - K_k \tilde{H}_k\right] \bar{P}_k \left[I - K_k \tilde{H}_k\right]^T + K_k R_k K_k^T \tag{25}$$

The LROE EKF formulation and measurement equations are presented. The derived form can be easily expanded to include additional dynamics perturbations. The advantage of using LROEs in the relative orbit estimation problem is the observability of the state.

Non-Dimensional LROE Set

One of the challenges with bearings-only estimation is the lack of observability of the full relative motion state.[4,9] The observability grammian

$$\mathcal{O}_N^T \mathcal{O}_N = H_0^T H_0 + \sum_{k=1}^{N} \Phi_{k-1,0}^T H_k^T H_k \Phi_{k-1,0} \tag{26}$$

provides the observability for the noise-free system. For the unperturbed LROE filter case this simplifies to

$$\mathcal{O}_N^T \mathcal{O}_N = \sum_{k=0}^{N} H_k^T H_k \tag{27}$$

For the angles-only relative motion sensing cases the unperturbed noise-free observability grammian for the LROE EKF is not full rank and thus the full LROE state suffers the classical lack of convergence as seen in other formulations. Consider the family of relative 2:1 ellipses as an example. The bearings measurement history is the same for the family of ellipses defined by scaling all LROE terms by a common constant. This lack of knowledge regarding the scale factor is what produces the rank deficient observability grammian.

To address this issue of estimating aspects of the relative motion with angles-only, a non-dimensionalized LROE set is defined by dividing all the elements by a reference LROE element. Note that since all non-singular LROE elements have units of distance, this non-dimensionalization is trivial to perform. Without loss of generality, the A_1 term is selected for scaling for the following examples to yield the reduced order 5×1 non-dimensional LROE set

$$\hat{\boldsymbol{X}} = \frac{1}{A_1} \begin{bmatrix} A_2 \\ B_1 \\ B_2 \\ x_{\text{off}} \\ y_{\text{off}} \end{bmatrix} = \begin{bmatrix} \hat{A}_2 \\ \hat{B}_1 \\ \hat{B}_2 \\ \hat{x}_{\text{off}} \\ \hat{y}_{\text{off}} \end{bmatrix} \tag{28}$$

The non-dimensionalized non-singular set generates a rank 5 observability grammian which demonstrates that the shape of the relative motion can be fully determined without knowing the scale factor. Including range information would resolve the relative motion scale factor. The non-dimensional measurement sensitivity matrix drops the non-dimensionalizing term, in this case the A_1 column, of Eq. (21) and the inputs are the non-dimensional positions $\hat{x}(t)$,$\hat{y}(t)$, and $\hat{z}(t)$ given by

$$x(t) = \cos(nt) - \hat{A}_2 \sin(nt) + \hat{x}_{\text{off}} \tag{29a}$$

$$y(t) = -2\sin(nt) - 2\hat{A}_2 \cos(nt) - \frac{3}{2} nt\hat{x}_{\text{off}} + \hat{y}_{\text{off}} \tag{29b}$$

$$z(t) = \hat{B}_1 \cos(nt) - \hat{B}_2 \sin(nt) \tag{29c}$$

This approach assumes that the non-dimensionalizing term is non-zero. If the filter does not know which terms are zero, a mixed-method of experts filtering approach would provide evidence of the correct formulation.

ILLUSTRATIVE LROE ESTIMATION CASES

The LROE extended Kalman filter formulation is implemented in a numerical simulation to demonstrate the feasibility of estimating the relative orbit shape without the scale information. The two satellites are inertially propagated with the full nonlinear two-body dynamics. The observations are extracted every 3 seconds using the true positions and are then altered by the addition of sensor noise. The filter propagates and estimates the LROE set and at each time step, the Gauss-Markov process is added to the LROE state. The continual perturbation of the LROE set help move the estimation of a constant towards the truth when the measurement noise begins to dominate the Kalman update. The measurement noise under-weighted to 5 times the true noise value. The chief spacecraft is initialized with a semi-major axis of 7500 kilometers and all other orbit elements as zero. The true relative orbit is initialized with $\boldsymbol{X}^{\text{true}}$ and the filter is given the initial conditions $\boldsymbol{X}^{\text{true}} + \Delta X$.

The filter covariance is given by $P_0 = 10^3 \times \text{diag}[1,\ 1,\ 1,\ 1,\ 0.1,\ 1]$ which is sufficiently large but is bounded by the 1 km range of applicability inherent in the CW equations. The true state process noise and the filter process noise is

$$Q^{\text{est}} \quad = \quad \text{diag}[3E^{-2},\ 3E^{-2},\ 3E^{-2},\ 3E^{-2},\ 1E^{-6},\ 1E^{-6}] \tag{30}$$

The magnitude of the process noise is sufficiently large such that the covariance bounds in the estimate encapsulate the state errors. The camera noise is defined in Eq. (15) and has a value of 1.5×10^{-4} radians. The LROE filter is applied to two cases: a drifting target and a relative ellipse. Both cases are not among the angles-only unobservable cases.

The LROE filter is applied to a drifting target satellite. The initial conditions and filter state error for the drifting case are

$$\boldsymbol{X}^{\text{true}} = \begin{bmatrix} A_1 \\ A_2 \\ B_1 \\ B_2 \\ x_{\text{off}} \\ y_{\text{off}} \end{bmatrix} = \begin{bmatrix} 100 \\ 0 \\ 200 \\ 0 \\ 20 \\ \text{-2.5} \end{bmatrix} [\text{m}] \qquad \Delta \boldsymbol{X} = \begin{bmatrix} 10 \\ \text{-2} \\ \text{-7} \\ 2 \\ 5 \\ \text{-5} \end{bmatrix} [\text{m}] \tag{31}$$

The true drifting relative orbit over the half-orbit simulation time is shown in Cartesian Hill frame coordinates in 2.

Relative Orbit Estimation using the Full Set of Dimensional LROE

Given the parameter values specified and the relative motion defined, the dimensional 6×1 LROE filter provides the state estimate and covariance shown in Figure 3. The final state estimate error after one orbit is $\boldsymbol{X}_{\text{error}} = [1.34,\ -0.11,\ 2.71,\ 0.08,\ 0.29,\ -0.08]$ meters. However, the error values are misleading as the solution is one of an infinite number of solutions because of the lack of observability. The lack of observability is visible in the continuous jitter in the estimate for the duration of the simulation. This example demonstrates that the LROE EKF cannot estimate the full 6×1 state uniquely using angles-only measurements. The second case uses the non-dimensional form to obtain the geometry without knowledge of the scale factor.

Relative Orbit Estimation using the Reduced Non-Dimensional LROE Set

A second simulation uses the same initial conditions and covariance as the previous case, but non-dimensionalizes the LROE with A_1. The following example shows the convergence to the un-

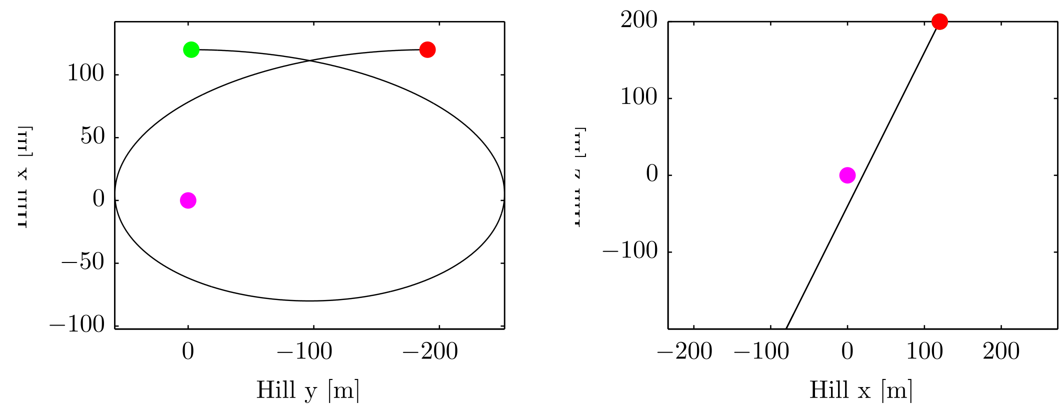

(a) Relative orbit, planar projection. (b) Relative orbit, XZ projection.

Figure 2. Hill frame relative orbit for the drifting relative ellipse example case. Start at o, finish at o about the chief.

scaled relative geometry. The final state estimate error after one orbit is already reduced to $\boldsymbol{X}_{\text{error}} = [0.01,\ 0.00002,\ 0.006,\ -0.00005,\ 0.02]$ meters. The results illustrate that a non-dimensional LROE EKF can estimate the relative motion shape using angles-only with increasing accuracy. This demonstrates the convenient geometric insight obtained when performing relative motion estimation using the LROEs.

CONCLUSIONS

The presented analytical development and numerical simulations show that a non-singular linearized relative orbit element (LROE) extended Kalman filter is capable of estimating the relative orbit shape using angles only measurements. The presented non-dimensional LROE approach in particular provides a full-rank estimation problem where the unobservable relative orbit scale information is elegantly excluded. Future work will apply the same LROE approach to a curvilinear set to remove linearization error and to address the range ambiguity.

ACKNOWLEDGEMENTS

The authors would like to thank the NASA Space Technology Research Fellowship (NSTRF) program, grant number NNX14AL62H, for support of this research.

REFERENCES

[1] S. D'Amico G. Gaias and J. S. Ardaens. Angles-only navigation to a noncooperative satellite using relative orbit elements. *Journal of Guidance, Control, and Dynamics*, 37(2), 2014.

[2] Eberhard Gill, Simone D'Amico, and Oliver Montenbruck. Autonomous formation flying for the prisma mission. *AIAA Journal of Spacecraft and Rockets*, 44(3):671–681, May–June 2007.

[3] Frank R. Chavez and T. Alan Lovell. Relative-orbit element estimation for satellite navigation and guidance. Providence, RI, August 16-19 2004. AIAA/AAS Astrodynamics Specialist Conference and Exhibit.

[4] Vincent J. Aidala and Sherry E. Hammel. Utilization of modified polar coordinates for bearings-only tracking. *IEEE Transactions on Automatic Control*, AC-28(3), March 1983.

[5] W. H. Clohessy and R. S. Wiltshire. Terminal guidance system for satellite rendezvous. *Journal of the Aerospace Sciences*, 27(9):653–658, Sept. 1960.

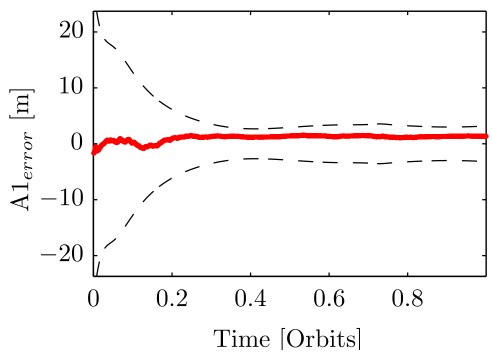

(a) A_1 state and 3σ variance.

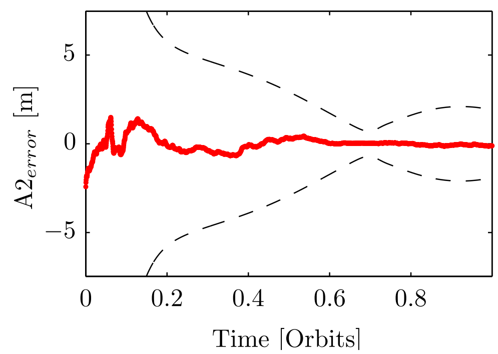

(b) A_2 state and 3σ variance.

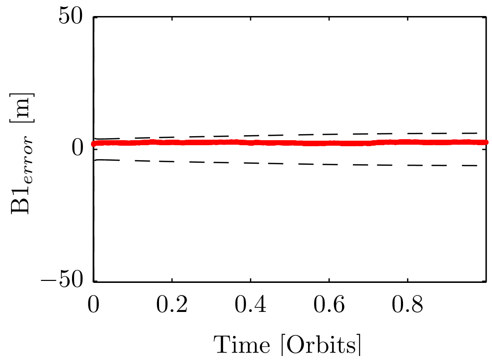

(c) B_1 state and 3σ variance.

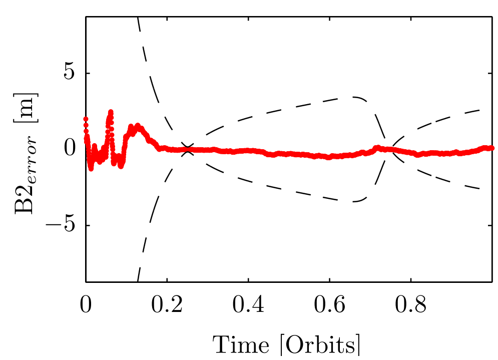

(d) B_2 state and 3σ variance.

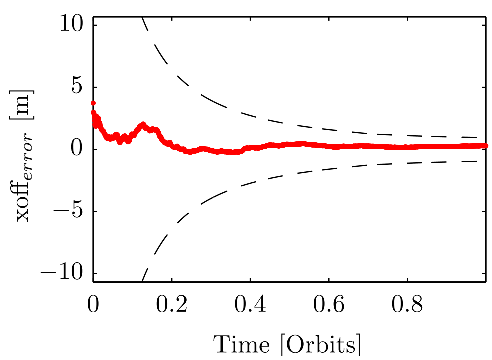

(e) x_{off} state and 3σ variance.

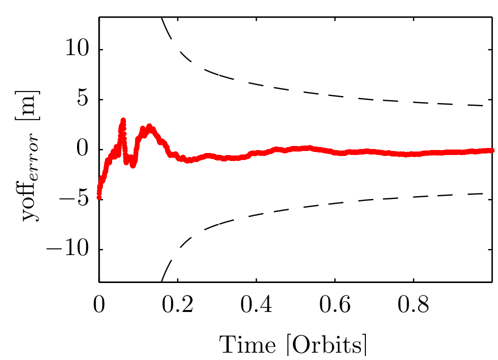

(f) y_{off} state and 3σ variance.

Figure 3. LROE estimated state error and covariance envelopes demonstrating the converging trend of the drifting relative ellipse estimate.

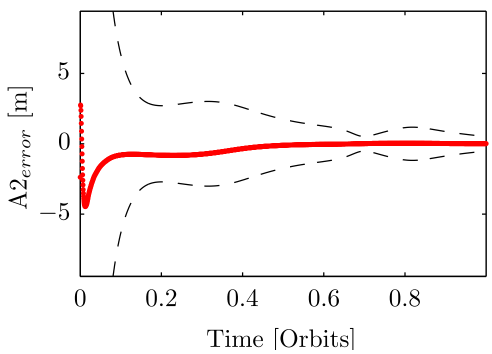

(a) A_2 state and 3σ variance.

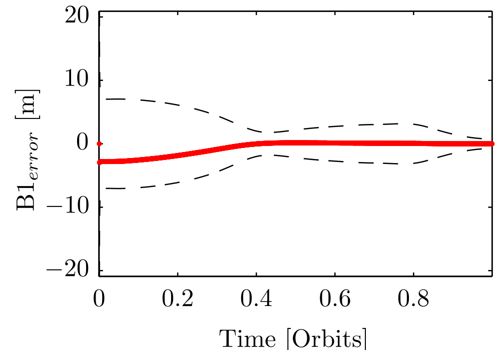

(b) B_1 state and 3σ variance.

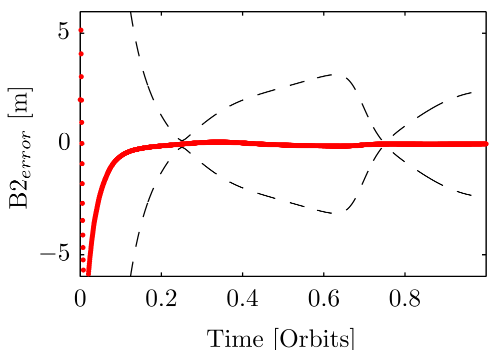

(c) B_2 state and 3σ variance.

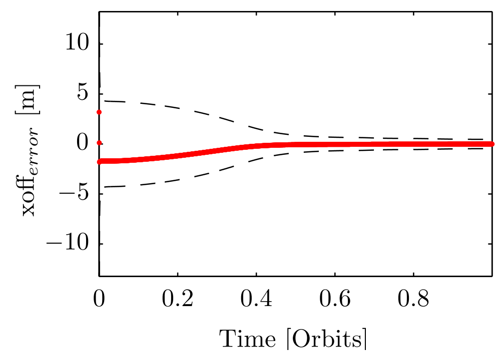

(d) x_{off} state and 3σ variance.

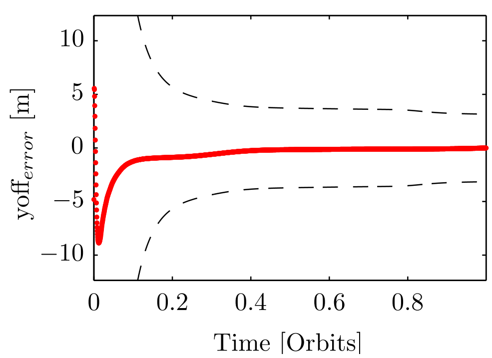

(e) y_{off} state and 3σ variance.

Figure 4. LROE estimated state error and covariance envelopes demonstrating the boundedness of the along-track offset relative ellipse estimate with large initial error.

[6] T. Alan Lovell and Steven G. Tragesser. Guidance for relative motion of low earth orbit spacecraft base on relative orbit elements. In *AIAA/AAS Astrodynamics Specialist Conference*, Providence, Rhode Island, August 16-19 2004.

[7] T. Alan Lovell, Steven G. Tragesser, and Mark V. Tollefson. A practical guidance methodology for relative motion of leo spacecraft base on the clohessy-wiltshire equations. In *14th AAS/AIAA Spaceflight Mechanics Meeting*, Maui, Hawaii, February 8–12 2004.

[8] S. D. Amico, E. Gill, and O. Montenbruck. Relative orbit control design for the prisma formation flying mission. In *AIAA Guidance, Navigation, and Control Conference and Exhibit*, August 21-24 2006.

[9] David C. Woffinden and David K. Geller. Observability criteria for angles-only navigation. *IEEE Transactions on Aerospace and Electronic Systems*, 45(3), July 2009.

[10] Alex C. Perez and T. Alan Lovell. Nonlinear representations of satellite relative motion equations using curvilinear transformations. In *AAS*, 2015.

[11] Thomas. A. Lovell and David A. Spencer. Relative orbital elements formulation based upon the clohessy-wiltshire equations. *Journal of Astronautics*, February 2015.

[12] T. Bennett and H. Schaub. Continuous-time modeling and control using linearized relative orbit elements. In *AAS/AIAA Astrodynamics Specialists Conference*, Vail, CO, August 9-13 2015.

[13] M. Humi and Thomas Carter. The clohessy-wiltshire equations can be modified to include quadratic drag. In *Proceedings of the AAS/AIAA Spaceflight Mechanics Meeting*, Ponce, Puerto Rico, Feb. 9–13 2003. Paper No. AAS 03–240.

[14] Carl R. Seubert and Hanspeter Schaub. Tethered coulomb structures: Prospects and challenges. *Journal of the Astronautical Sciences*, 57(1-2):347–368, Jan.–June 2009.

[15] Oliver Montenbruck. An epoch state filter for use with analytical orbit models of low earth satellites. *Aerospace Science and Technology*, pages 277–287, 2000.

[16] F. Landis Markley and J. Russell Carpenter. Linear covariance analysis and epoch state estimators. *NASA Goddard Space Flight Center*.

[17] S. D. Amico, J. S. Ardaens, and R. Larsson. In-flight demonstration of formation control based on relative orbit elements. In *4th International Conference on Spacecraft Formation Flying Missions and Technologies*, August 18-20 2011.

[18] Jeremy Schwartz and Tom Krenzke. Error-contracting impulse controller for satellite cluster flight formation. In *AIAA Guidance, Navigation and Control Conference*, Boston, MA, August 19-22 2013.

[19] Sean Chalt and David A. Spencer. Prox-1: Automated trajectory control for on-orbit inspection. In *37th Annual American Astronautical Society Guidance and Control Conference*, January 2014.

[20] Hanspeter Schaub and John L. Junkins. *Analytical Mechanics of Space Systems*. AIAA Education Series, Reston, VA, 2nd edition, October 2009.

[21] David A Vallado. *Fundamentals of Astrodynamics and Applications*. Microcosm Press, 4th edition, March 2013.